



Preparation and Characterization of High Specific Surface Area γ -Alumina Nanoparticles Via Sol-Gel Method

S.M. Siahpoosh, E. Salahi*, F. Alikhani Hessari, I. Mobasherpour

Materials and Energy Research Center (MERC), Karaj, Iran.

PAPER INFO

Paper history:

Received 10 March 2017

Accepted in revised form 30 December 2017

Keywords:

γ -Alumina

Nanoparticles

Sol-Gel

Aluminum Isopropoxide

Textural Properties

ABSTRACT

In the current investigation, γ -alumina nanoparticles with sizes less than 10 nm, high specific surface area (351 m²/g), high pore volume and relatively narrow pore size distribution were prepared via the sol-gel method in presence of aluminum isopropoxide as an aluminum precursor, distilled water, acetic acid as hydrolysis rate controller and tert-butanol as solvent. They had meso and macro porosities in which most of the pores were cylindrical. The as-dried powder was analyzed by simultaneous thermal analysis (STA) method. The calcined γ -alumina nanoparticles were analyzed using X-ray diffractometer (XRD), field emission scanning electron microscopy (FESEM), Fourier transform infrared spectroscopy (FTIRs), and nitrogen adsorption-desorption techniques. This study revealed that the precursor and solvent types, weight ratios of reactants, calcination temperatures and times are important factors for preparation of γ -alumina with high surface area and well defined narrow pore size distribution for heavy metals adsorption.

1. INTRODUCTION

Performance of different alumina compounds, especially α -alumina, was investigated in many researches and various results have been reported, but properties of γ -alumina have not been studied as frequently as others [1]. The usefulness of γ -alumina relies on favorable combination of physical and textural properties (e.g. density, surface area, pore volume and pore size distribution); thermal properties (e.g. thermal and hydrothermal stability); and chemical properties (e.g. acid-base characteristics). New methods to produce porous γ -alumina are making possible its application in catalytic process, ultrafiltration membranes, liquid chromatography technique, fluorosis prevention, and treatment of aqueous effluents containing heavy metals [2].

Nowadays preparation of nanostructures using methods such as hydrolysis, thermal decomposition, chemical vapor deposition, and sol-gel has gained significant importance [3, 4]. Wang et al., [5] prepared alumina nanofibers by hydrolyzing aluminum nitrate in presence of hexamethylenetetramine. Rajendran and Bhattacharya [6] used sol-gel emulsion method to

obtain thermally stable alumina spheres with diameter less than 1 μ m.

Samples prepared through traditional preparation methods, possess relatively low surface area (less than 200 m²/g) and broad pore size distribution which limit the catalytic activity of alumina in various applications [7]. Despite the presence of many researches about the synthesis of mesoporous γ -alumina, there are challenges to develop a facile and surfactant-free solution route for preparation of these materials by using non-traditional methods.

Properties of γ -alumina are largely dependent on properties of boehmite. So to obtain controllable and desired γ -alumina, many efforts have been done for preparation of boehmite with different morphologies and microstructures.

G. Jian-feng et al., [8] and Shen et al., [9] used aluminum nitrate as the precursor and in another research D. Ma et al., [10] used aluminum chloride precursor and produced boehmite and γ -alumina nanoparticles through the hydrothermal method and their main limitation was the lack of high-purity powder. J. Mullens et al., [11] prepared boehmite and γ -alumina platy nanoparticles with the same method by using aluminum alkoxide precursor and achieved particles with high purity and low levels of agglomeration in the range of 30-80 nm. In another

*Corresponding Author's Email: e-salahi@merc.ac.ir (E. Salahi)

study, Y. Zhai [12] examined γ -alumina preparation by ethanol precipitation. Results indicated that ethanol would prevent from creation of agglomerates in the deposition. Palkar [13] obtained porous spheres of γ -alumina with 0.5 mm diameter through sol-gel process. Also, Santos et al., [2] provided macroporous γ -alumina based on the gel process with or without the presence of soot and saw dust.

According to researches, the final product of the sol-gel method has high purity and surface energy. The procedure for achieving small sized particles is by using solution conditions and having low temperature during the heat treatment [14]. On the other hand, even though aluminum isopropoxide precursor is not completely soluble in ethanol [11], it is the most commonly-used solvent for preparation of γ -alumina nanoparticles via the sol-gel method. Effects of other solvents on the textural and morphological properties of γ -alumina in the presence of this precursor and acidic catalyst have not been studied thoroughly.

So, the sol-gel method is used in this research after investigating the effects of various solvents on preparation of γ -alumina nanoparticles with specific surface area higher than 350 m²/g, high pore volume and appropriate pore size distribution for heavy metal adsorption in presence of tert-butanol solvent.

2. MATERIALS METHOD

2.1. Starting materials

Preparation of γ -alumina nanoparticles was done via sol-gel method with cheap and high purity raw materials and without environmental pollution. Aluminum isopropoxide alkoxide was used as aluminum precursor instead of aluminum inorganic salts which produces γ -alumina powder with a higher specific surface area. This material is cheaper and easily available compared to many other alkoxides such as tri-sec-butoxide aluminum. Aluminum isopropoxide (AIP, Al(OCH(CH₃)CH₃)₃, >98.0 wt%, MERCK Art. No. 801079), tert-butanol ((CH₃)₃COH, >99.0 wt%, MERCK Art. No. 822264), and acetic acid (AA, CH₃CO(OH), >63.0 wt%, MERCK Art. No. 62) were used as starting materials. In all preparation stages, distilled water was used. All Materials were of analytical grade and were used without further purification.

2.2. Synthesis of γ -Alumina

All experiments were conducted under air atmosphere. Aluminum isopropoxide was used as aluminum precursor, acetic acid as hydrolysis rate controller and tert-butanol as solvent during the synthesis procedure. During the processing, weight ratios of the reactants AIP: Solvent, AIP: H₂O, and AIP: AA were 1:60, 1:1, and 40:1, respectively. Initially, 0.065 molar AIP solution was prepared under continuous and vigorous

magnetic stirring at 150 rpm for 3 hours at room temperature. Then, the mixture of 0.07 ml acetic acid and 3 ml of distilled water was added drop-wise into the above solution. The solution was magnetically stirred for 3 hours for completion of the hydrolysis.

After adding the two solutions, the final solution was placed in a glass vessel at room temperature for 24 hours and resulted in formation of a gel. The gel was dried in an oven at 120°C for 6 hours in flow of air. A white dry gel was obtained which was pulverized and passed through 70-mesh sieve.

Heat treatment for powder calcination took place in a normal environment, using a laboratory chamber furnace which is equipped with thermal string of silicon carbide and is able to reach 1500°C as its maximum temperature. The sample was poured in an alumina crucible and was heated to 600°C with ramp rate of 2°C/minute. It was maintained at that temperature for 6 hours so that γ -alumina white powder was obtained after slow and gradual cooling step in the furnace. A ramp rate of 2°C/min was used to (1) avoid rapid dehydration to ensure uniform pore construction and (2) ensure uniform heat transfer to achieve better homogeneity and avoid rapid grain growth [1].

Reactivity of the precursors depends on their chemical properties [15]. Aluminum isopropoxide is sensitive to moisture and even air moisture is sufficient for hydrolysis reaction. The performed final reaction at low temperature is shown in following:



In this reaction, R is the propyl group (–C₃H₇). Accordingly, the hydrolysis reaction is done completely due to high water content and high tendency of the aluminum isopropoxide to react with water. As expected, using aluminum isopropoxide precursor in solution leads to formation of propylene glycol as a by-product of the reaction. This compound is decomposed and came out of the system during calcination of prepared powder; without undesirable effects on the final product.

2.3. Characterization

2.3.1. Differential thermal and thermogravimetric analysis (DTA/TGA)

To discover various decomposition steps occurring in as-dried powder as a function of temperature, and to determine proper temperature of calcination process, differential thermal and thermogravimetric analysis instrument was used (BÄHR, STA-503, Germany). Determining this temperature is important; for the less, lower degree of γ -alumina crystallinity, lower particle size and greater specific surface area would be achieved. Also increasing the calcination temperature allows arising the other impurity phases in the samples. For this experiment, approximately 9.93 mg of as-dried boehmite powder was loaded on an alumina pan and

was heated along with commercial alumina as the reference material, from room temperature to 1200°C under the air atmosphere with a ramp rate of 10°C/minute until no weight loss occurred.

2.3.2. X-ray diffraction (XRD)

Phase identification and crystallinity of the sample were assessed by X-ray diffraction using Siemens D-500, semi-automatic, at room temperature with Cu-K α radiation ($\lambda = 1.5404 \text{ \AA}$). The sample diffraction intensity is measured in the Bragg angle (2θ) range between 20-80°, second residence time per step and 0.02 degrees of step size for each point were employed. The data is collected with sample rotation. It is noteworthy that Cu-K α radiation is obtained from a copper X-ray tube operated at 30 kV and 25 mA. Obtained phases are identified by comparing the diffraction angle of XRD peaks with the corresponding intensity values in the ASTM cards and PANalytical X'pert High Score Plus software, 2.2b version-2006-11-01 release date. The full width at half maximum (FWHM) is determined accurately after correcting the instrument broadening and the crystallite size is then estimated by using Scherer equation in nanometer [16]:

$$D_{\text{XRD}} = \frac{0.94\lambda}{\beta \cos\theta} \quad (2)$$

where λ is the wavelength of the incident radiation, β is the full width of diffraction peak at half maximum intensity (FWHM) and θ is the diffraction angle. This equation can be used when the crystallite size is less than 1000 Å. In order to determine the crystallite size, the peaks of the planes with the maximum intensity are used as they have clear and appropriate separation which is better than other peaks.

2.3.3. Nitrogen gas adsorption/desorption

The specific surface area, total pore volume, average pore diameter and the of pore diameter size distribution of the calcined powder were measured using nitrogen gas adsorption/desorption isotherm at liquid nitrogen temperature (77.4 K) by using Belsorp instrument (mini-II version). The pore volumes were determined at a relative pressure $P/P_0 = 0.99$. Specific surface area was calculated using the Brunauer-Emmett-Teller (BET) equation, at P/P_0 range between 0.05–0.35. It should be noted that P and P_0 are partial pressure in the adsorbed gas by Pascal in equilibrium and experimental conditions, respectively. Pore size distribution of powder was obtained employing the Barrett-Joyner-Hatenda (BJH) model (N $_2$ gas adsorption on silica as reference). The as-prepared sample was degassed at 150°C in a vacuum flow for 12 hours to remove the water and any impurities physisorbed on the solid surface. In this study, adsorption of nitrogen gas is expressed by the isotherms which are equivalent to amount of adsorbed material on surface of adsorbent

[17]. On the contrary, desorption isotherms are obtained by measuring amount of desorbed gas. Isotherms of I, II, and III type are usually reversible, but I type could have a hysteresis loop. The hysteresis loop also can be seen in types of IV and V. The hysteresis loop indicates presence of meso pores in the material and helps to achieve some information about geometry of pores. Assuming sphericity and same size of the particles, the measured specific surface area for the sample in crystallite forms was converted to equivalent particle size according to Equation (3) [18]:

$$D_{\text{BET}} = \frac{6000}{\rho \cdot S_{\text{BET}}} \quad (3)$$

where D_{BET} is average particle size in nm, S_{BET} is specific surface area expressed in m 2 /g and ρ the theoretical density expressed in g/cm 3 .

2.3.4. Field emission scanning electron microscopy (FESEM)

FESEM images were obtained with a TESCAN-MIRA3 scanning microscope operated at an acceleration voltage of 10 kV and were used to study the surface of the sample. To determine the elements in sample, the energy dispersive X-ray spectroscopy (EDS) was used for prepared powders using microscope ancillary facilities.

2.3.5. Fourier transform infrared spectroscopy (FTIRs)

Infrared spectroscopy is an important tool in identification of functional groups that might exist in different substances. FTIR spectra of dispersed samples on KBr disks were recorded at room temperature using Perkin Elmer spectrometer (Spectrum 400, United States) in the range of 4000 to 400 cm $^{-1}$ at a resolution of 4 cm $^{-1}$ and 30 scans for each run. Disks were dried at 373 K for 24 hours prior to recording the FTIR spectrum.

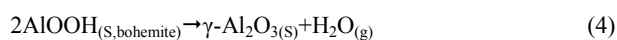
3. RESULT AND DISCUSSION

3.1. Thermal analysis

In this study, DTA/TGA profiles provide insights into the phase transition from boehmite to γ -alumina. The DTA/TGA curves of as-dried boehmite powder during processing are shown in Fig. 1.

The DTA curve presents three major peaks and two of them are endothermic and another one is exothermic. In the TGA curve of as-dried boehmite powder, there are three stages of decomposition reaction with a total weight loss of ~45%. The initial stage corresponds to an endothermic weight loss of ~20% which is attributable to remove of physically adsorbed water and residual moisture from room temperature to 200°C. The second weight loss, between 200°-500°C is an exothermic process that occurs due to decomposition of organics

including adsorbed acetic acid and the removal of chemically adsorbed water molecules. It should be noted that decomposition temperature of acetic acid is about 440°C. The third stage which comes with appearance of exothermic broad peak, happens above 500°C which is attributable to a weight loss due to the crystallization of transition alumina, oxidation of organic volatile residues, elimination of OH groups, and slow continuous dehydroxylation. Total weight loss in the last two stages is ~25%. TGA curve is flat at temperatures of about 600°C and it can be seen that there is no significant weight loss at higher temperatures; Meaning that the organic residues have been removed completely and the sample has reached a stable structure. Therefore, calcination process is suitable at temperature of about 600°C. The above described process can be summarized in following dehydration reaction [19]:



According to the reaction, calculated theoretical value for ultimate weight loss of produced γ -alumina is 15% that is much less than the actual experimental weight loss. This indicates presence of significant amounts of alcohol molecules that are adsorbed physically or chemically on the surface of precursor and are removed with increasing the temperature.

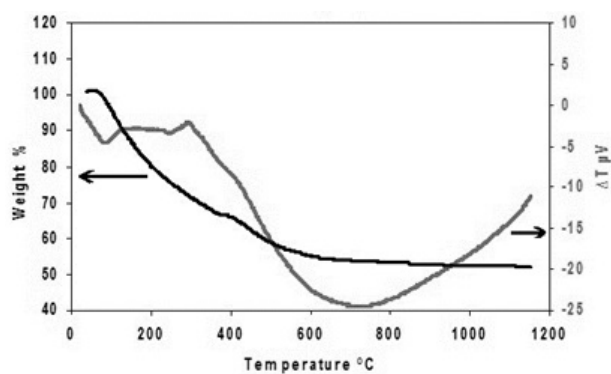


Figure 1. DTA/TGA curves of the as-dried boehmite powder

According to the data reported by Valente et al., [20] and Woodfield et al., [1] transition from boehmite to γ -alumina takes place in the temperature range of 400–700°C; their results are in accordance with thermal analysis of present report, since thermal treatment of powder at 600°C led to formation of γ -alumina.

3.2. X-ray diffraction

The crystalline nature of the as-dried boehmite and γ -alumina prepared with aluminum isopropoxide in presence of tert-butanol alcoholic solvent was studied by X-ray diffraction. The resulting patterns in high-angle diffraction are shown in Fig. 2. Fig. 2(a) shows

characteristic peaks of boehmite (JCPDS card 04-013-2972). The five main peaks at 2θ angles around 28, 38, 49, 67, and 73° can be indexed as (120), (140), (051), (231), and (251) planes, respectively. Also, the five main reflections of γ -alumina phase (JCPDS card 00-029-0063) are clearly observed (Fig. 2(b)) as broad peaks at 2θ angles around 32, 37, 40, 46, and 66° which correspond to (220), (311), (222), (400), and (440) planes, respectively.

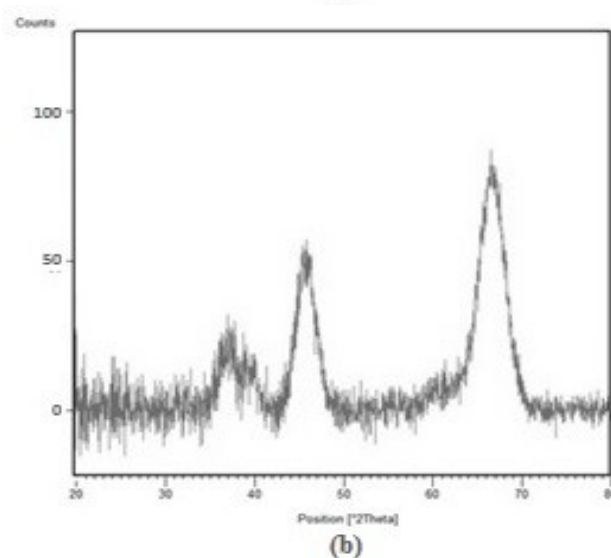
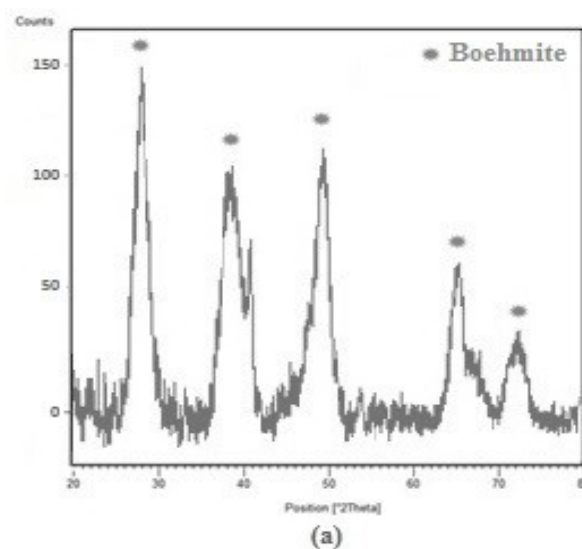


Figure 2. X-ray diffraction pattern at high angles diffraction for the (a) as-dried boehmite (b) prepared γ -alumina

Diffraction peaks in XRD patterns were broad because crystallites were very small. Such sizes indicate their partly weak crystalline nature in the boehmite and γ -alumina. It should be noted that no peak of other phases of alumina can be recognized in diffraction pattern of calcined sample and the only detectable phase is γ -alumina.

The calculation is done for γ -alumina based on Scherrer equation in (440) planes with the maximum intensity of diffraction and 2θ angle of 66° . The average obtained crystallite sizes (D_{XRD}) is 5.4 nm which represents the nanometer structure.

3.3. Textural properties

Textural properties such as total pore volume, average pore diameter, specific surface area and average particle size of the γ -alumina are investigated using BET analysis. These are presented in Table 1.

TABLE 1. Textural properties of the prepared γ -alumina

Specific surface area (m ² /g)	Total pore volume (cm ³ /g)	Average pore diameter (nm)	Average particle size (nm)
351	1.09	12.43	5.34

The nitrogen adsorption/desorption isotherm of the sol-gel derived γ -alumina is shown in Fig. 3.

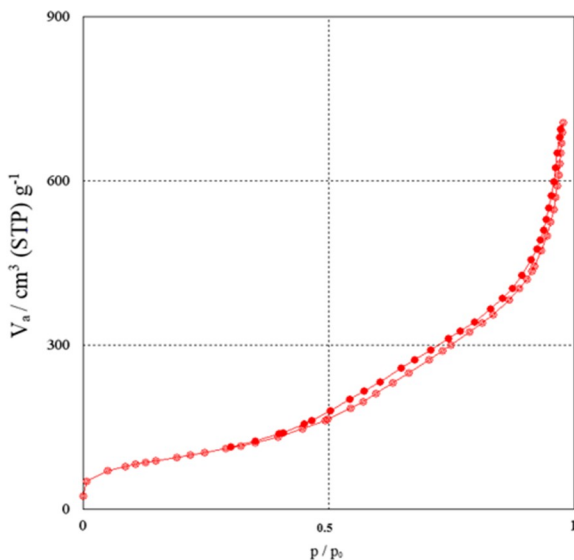


Figure 3. Nitrogen adsorption/desorption isotherm for the prepared γ -alumina

According to IUPAC classification, the isotherm obtained for the sample is characterized as V type. This isotherm has been extended in almost flat and stretched conditions until high relative pressures which is characteristic of mesoporous solids, is reached. In addition, significant slope changes occurred in the curve at high relative pressures of about $P/P_0 = 0.9$ which indicates presence of some macro pores in structure of the sample.

The shape of hysteresis loops can be correlated with the changes in pore structure, which in this case can be a phase transformation from boehmite to γ -alumina with different morphologies [17]. In this study, hysteresis loop for the prepared γ -alumina occurred at a relative

pressure range of $P/P_0 = 0.35-0.98$. It is H1 type showing that adsorption and desorption branches have completely parallel mode, so most of the pores are in cylindrical shape. Ultimate amount of nitrogen adsorbed by sample was more than 600 cm³/g, indicating presence of large volume pores.

Fig.4 shows pore-size distribution of the prepared γ -alumina employing BJH model. It indicates relatively narrow and uniform distribution of micro and meso pores with 1–10 nanometer sizes in the sample, where related maximum peak is seen in 2.1 nm. Based on the previous researches, textural properties of materials including high specific surface area, large pore volume and a narrow pore-size distribution in the range of 1 to 10 nm are of great interest for both adsorption and catalytic applications [17].

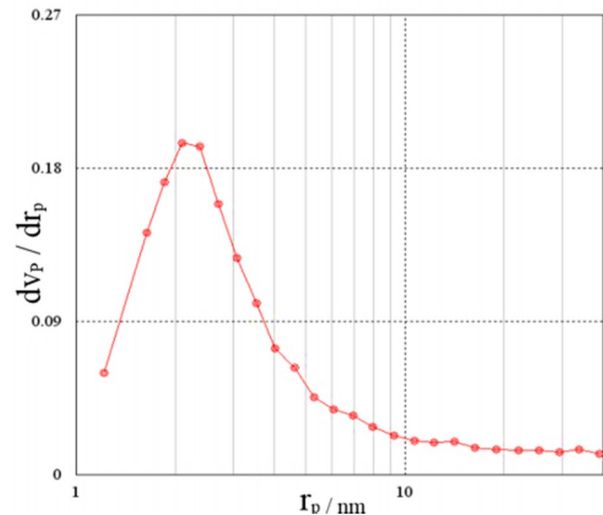


Figure 4. BJH model of the prepared γ -alumina

3.4. Morphology

Figs. 5 and 6 show FESEM images of the as-dried boehmite and prepared γ -alumina, respectively. As shown, the samples have spongy structure and are composed of porous and homogenous aggregates with different sizes. These aggregates possess nanoparticles with sizes less than 10 nm. The results are in accordance with the particle sizes of prepared γ -alumina which were estimated by BET data.

EDS analysis results of the prepared γ -alumina nanoparticles which are shown in Fig. 7 confirmed the presence of aluminum and oxygen ions. It is noteworthy that presence of carbon and gold peaks were related to the substrate of carbon and the metal used for analysed powder coating, respectively.

3.5. Fourier transform infrared spectroscopy

Fig. 8 shows FTIR spectrum of the γ -alumina nanoparticles recorded in KBr pellet. The strong broadening band at 3800–3000 cm⁻¹ occurs due to the hydrogen bond between the various hydroxyl groups in the γ -alumina nanoparticles.

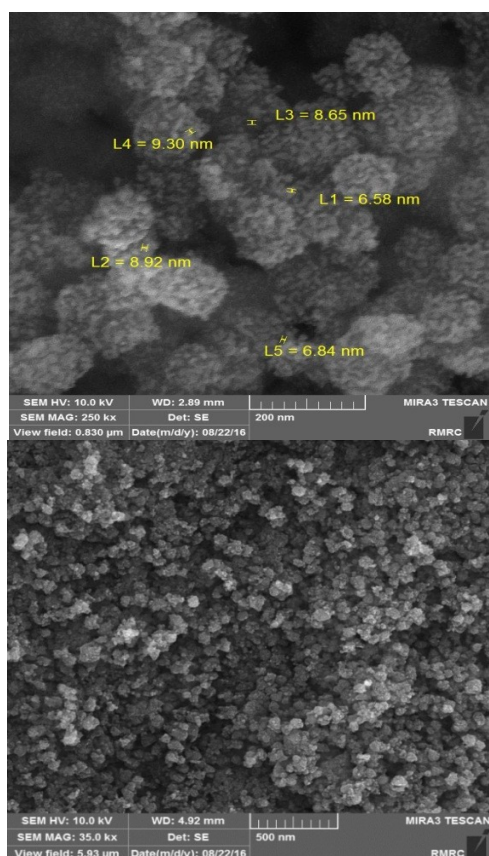


Figure 5. FESEM image of the as-dried boehmite

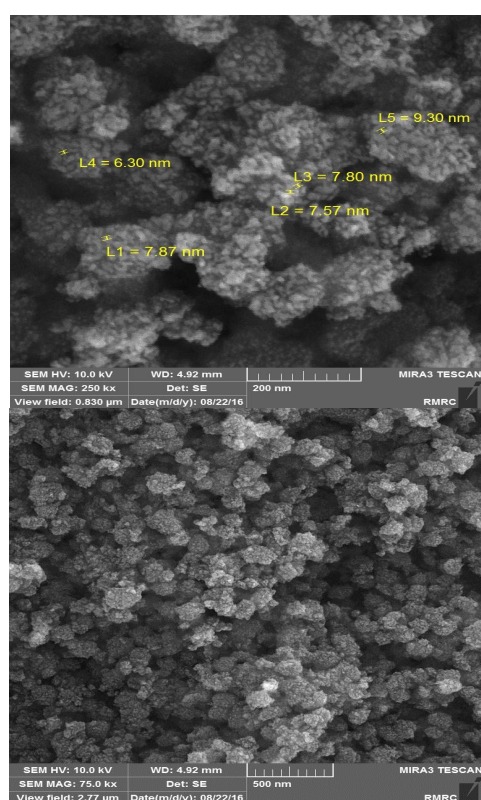


Figure 6. FESEM image of the prepared γ -alumina

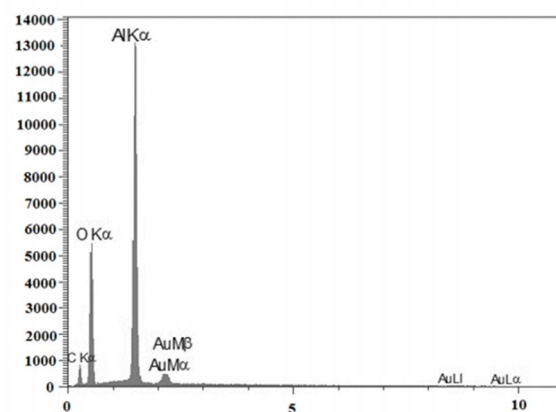


Figure 7. EDS diagram of the prepared γ -alumina

Another broadening band at $1000\text{--}400\text{ cm}^{-1}$, corresponds to Al–O vibration. The broad –OH stretching adsorption band which appeared at 3473.02 cm^{-1} , reveals presence of hydroxyl groups. The weak peak at 1635.33 cm^{-1} is related to the bending mode of adsorbed water. Peaks in the range of $1600\text{--}1400\text{ cm}^{-1}$ belong to –OH group's vibrations and impurities. The broad adsorption band at 798.84 cm^{-1} and the peak in range of $700\text{--}500\text{ cm}^{-1}$ represent stretching mode of AlO_4 and AlO_6 , respectively. So, prepared γ -alumina nanoparticles have both tetrahedral and octahedral positions. It is also expected that Al–O–H bending mode is in range of $1200\text{--}900\text{ cm}^{-1}$. It is seen that there is a strong peak at 1084.05 cm^{-1} and a small hump at 1164 cm^{-1} which belong to symmetrical and asymmetrical Al–O–H bending modes, respectively. These results are well in accordance with the FTIR spectrum of γ -alumina in other researches [21, 22].

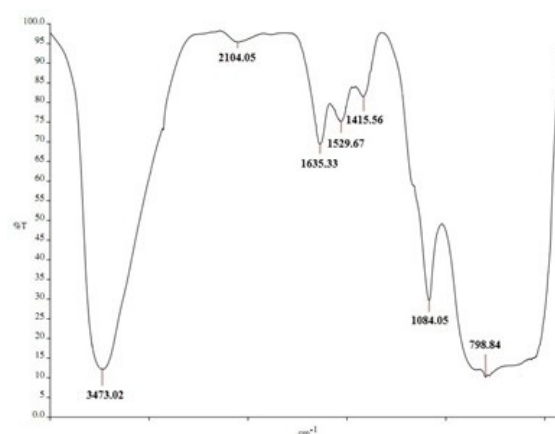


Figure 8. FTIR spectra of the prepared γ -alumina

3.6. Proposed mechanism for γ -Alumina nanoparticles formation with high specific surface area

A sol-gel transfer reaction between precursor and solvent molecules may eventually affect the cross-

linking mechanism in void regions of different sizes within the gel network.

In the present study, sol particles of boehmite are formed through hydrolysis and condensation reactions. Slower hydrolysis and faster condensation lead to formation of polymeric chains with high cross-linking and branching [14]. Enhanced cross-linking in gel networks results in formation of larger voids regions which is in agreement with the observed higher specific surface area, larger total pore volume, and the significant mesoporosity of the final products. On the other hand, discontinuity of gel network may be referred to encapsulating of sol particles of boehmite in primary solution during drying process and solvent evaporation. In these conditions, specific surface area of the prepared γ -alumina depends on extent of aggregation and dissolution of gel grains; so that aggregation of gel grains leads to formation of γ -alumina nanoparticles with higher specific surface area, and dissolution and decomposition of them lead to formation of γ -alumina nanoparticles with lower specific surface area [23]. In acidic conditions, the encapsulated alkoxide particles are decomposed upon calcination and resulting in further porosity, which may explain the formation of the γ -alumina nanoparticles prepared from alkoxide. This mechanism supports the formation of mainly mesopores with smaller average diameter and the absence of the noticeable amount of macro pores in the prepared γ -alumina nanoparticles, in presence of tert-butanol as solvent. In this sample, pores were homogeneous and the final aggregates were ordered. This can be attributed to formation of small and homogeneous sol particles of boehmite.

Acetic acid plays a crucial role in controlling the γ -alumina nanoparticles' microstructure due to moderate boehmite particles growth speed in different modes. That is probably through its selective adsorption on high-energy faces of boehmite particles during the ageing process [24]. In these conditions, high energy levels would not be available for growth and therefore crystal growth speeds are reduced significantly because of strong interaction between CH_3COO groups of acetic acid and boehmite particles with high energy levels. On the other hand, due to gradually nucleation of boehmite during the ageing process, where no adsorption of acetic acid takes place, energy levels are minimized and boehmite nanoparticles are formed with specified morphology.

4. CONCLUSION

The present study was successful in synthesizing porous γ -alumina nanoparticles using a facile sol-gel method. The γ -alumina prepared in presence of tert-butanol as a solvent even after calcining process of boehmite at 600°C , had specific surface area of $351 \text{ m}^2/\text{g}$, pore volume of $1.09 \text{ cm}^3/\text{g}$, particle size of 5.34 nm , and

suitable pore size distribution which are desirable for heavy metal adsorption.

5. ACKNOWLEDGMENTS

The authors are grateful to the Materials and Energy Research Center (MERC) and the Iranian Nanotechnology Initiative Council for their financial support for this study.

REFERENCES

- Huang, B., Bartholomew, C. and Woodfield, B.F., "Facile synthesis of mesoporous γ -alumina with tunable pore size: The effects of water to aluminum molar ratio in hydrolysis of aluminum alkoxides", *Microporous and Mesoporous Materials*, Vol. 183, (2014), 37-47.
- Faria, C.L.L., Oliveira, T.K.R., Santos, V.L., Rosa, C.A., Ardisson, J.D., Macêdo, W.A. and Santos, A., "Usage of the sol-gel process on the fabrication of macroporous adsorbent activated-gamma alumina spheres", *Microporous and Mesoporous Materials*, Vol. 120, (2009), 228-238.
- Jun, Y.W., Choi, J.S. and Cheon, J.W., "Shape Control of Semiconductor and Metal Oxide Nanocrystals through Nonhydrolytic Colloidal Routes, A review", *Angewandte Chemie International Edition in English*, Vol. 45, (2006), 3414-3439.
- Zou, G.F., Li, H., Zhang, Y.G., Xiong, K. and Qian, Y.T., "Solvothermal/hydrothermal route to semiconductor nanowires", *Nanotechnology*, Vol. 17, (2006), S313.
- Wang, J., Wang, Y., Qiao, M., Xie, S. and Fan, K., "A novel sol-gel synthetic route to alumina nanofibers via aluminum nitrate and hexamethylenetetramine", *Materials Letters*, Vol. 61, (2007), 5074-5077.
- Rajendran, M. and Bhattacharya, A.K., "A process for the production of sub-micron to millimetre sized thermally stable α -alumina spheres", *Materials Science and Engineering: B*, Vol. 60, (1999), 217-222.
- Masuda, H., Higashitani, K. and Yoshida, H., "Powder Technology: Handling and Operations, Process Instrumentation and Working Hazards", CRC Press, (2006).
- Jian-hong, Y., You-yi, S., Jian-feng, G. and Chun-yan, X., "Synthesis of crystalline $\gamma\text{-Al}_2\text{O}_3$ with high purity", *Transactions of Nonferrous Metals Society of China*, Vol. 19, (2009), 1237-1242.
- Shen, S.C., Ng, W.K., Chen, Q., Zeng, X.T. and Tan, R.B.H., "Novel synthesis of lace-like nanoribbons of boehmite and γ -alumina by dry conversion method", *Materials Letters*, Vol. 61, (2007), 4280-4282.
- Liu, Y., Ma, D., Han, X., Bao, X., Frandsen, W., Wang, D. and Su, D., "Hydrothermal synthesis of microscale boehmite and gamma nanoleaves alumina", *Materials Letters*, Vol. 62, (2008), 1297-1301.
- Lepot, N., Van Bael, M.K., Van den Rul, H., D'Haen, J., Peeters, R., Franco, D. and Mullens, J., "Synthesis of platelet-shaped boehmite and γ -alumina nanoparticles via an aqueous route", *Ceramics International*, Vol. 34, (2008), 1971-1974.
- Wang, S., Li, X., Wang, S., Li, Y. and Zhai, Y., "Synthesis of $\gamma\text{-Al}_2\text{O}_3$ via precipitation in ethanol", *Materials Letters*, Vol. 62, (2008), 3552-3554.
- Palkar, V.R., "Sol-gel derived nanostructured γ -Alumina porous spheres as an adsorbent in liquid chromatography", *Nano Structured Materials*, Vol. 11, (1999), 369-374.

14. Brinker, C. and Scherer, G., "Sol-Gel Science", Academic Press, (1989).
15. Burgos, M. and Langlet, M., "The sol-gel transformation of TIPT coatings: a FTIR study", *Thin Solid Films*, Vol. 349, (1999), 19-23.
16. Cullity, B.D. and Stock, S.R., "Elements of X-Ray Diffraction", Prentice Hall, U.S.A, (2001).
17. Lowell, S. and Shields, J.E., "Powder Surface Area and Porosity", Chapman and Hall, London and New York, (1984).
18. Hosseini, Z., Taghizadeh, M. and Yaripour, F., "Synthesis of nanocrystalline γ -Al₂O₃ by sol-gel and precipitation methods for methanol dehydration to dimethyl ether", *Natural Gas Chemistry*, Vol. 20., (2011), 128-134.
19. Asencios, Y.J.O. and Sun-Kou, M.R., "Synthesis of high-surface-area γ -Al₂O₃ from aluminum scrap and its use for the adsorption of metals: Pb(II), Cd(II) and Zn(II)", *Applied Surface Science*, Vol. 258, (2012), 10002-10011.
20. Valente, J., Bokhimi, X. and Toledo, J., "Synthesis and catalytic properties of nanostructured aluminas obtained by sol-gel method", *Applied Catalysis A*, Vol. 264, (2004), 175-181.
21. Zeng, Z., Yu, J. and Guo, Z.X., "Preparation of functionalized core-shell alumina/polystyrene composite nanoparticles", *Macromolecular Chemistry and Physics*, Vol. 206, (2005), 1558-1567.
22. Busca, G., Lorenzelli, V., Ramis, G. and Willey, R.J., "Surface sites on spinel-type and corundum-type metal oxide powders", *Langmuir*, Vol. 9, (1993), 1492-1499.
23. Hellgardt, K. and Chadwick, D., "On the preparation of high surface area aluminas from nitrate solutions", *Industrial and Engineering Chemistry Research*, Vol. 37, (1998), 405-411.
24. Deshpande, S.B., Potdar, H.S., Kholam, Y.B., Patil, K.R., Pasricha, R. and Jacob, N.E., "Room temperature synthesis of mesoporous aggregates of anatase TiO₂ nanoparticles", *Materials Chemistry and Physics*, Vol. 97, (2006), 207-212.